NILU METreport

Deposition of sulfur and nitrogen in Norway 2017-2021

Lewis R. Blake, Wenche Aas, Bruce Denby, Anne Hjellbrekke, Qing Mu, David Simpson, Martin Ytre-Eide and Hilde Fagerli

METreport

Title	Date
Deposition of sulfur and nitrogen in Norway 2017-2021	April 24, 2023

Institutes	Report no.
[1]Meteorological Institute, Oslo, Norway [2]The Climate and Environmental Research Institute NILU, Kjeller, Norway	03/2023

Author(s)	Classification
Lewis R. Blake[1], Wenche Aas[2], Bruce Denby[1], Anne Hjellbrekke[2], Qing Mu[1], David Simpson[1], Martin Ytre-Eide[2] and Hilde Fagerli[1]	● Free ○ Restricted

Client(s)	Client's reference
Norwegian Environment Agency, Oslo, Norway and Sub-contractor to NIVA – Norwegian Institute for Water Research, Oslo, Norway	Responsible at the Norwegian Environment Agency is Gunnar Skotte

Abstract This report contains estimates of atmospheric deposition of major inorganic compounds in Norway for the period 2017 to 2021 using two different methods, one observational based method while the other combining atmospheric transport model with observations. Both methods show similar clear spatial gradient in the atmospheric deposition with highest loads in south and south-west. The combined method has improved the spatial information of the deposition pattern for wet deposition. Compared to the previous period 2012-2016, there is a decrease in the total deposition of both sulfur and nitrogen in Norway.

Keywords

Long-range transport of air pollutants, Acid rain and eutrophication, Fusion

H. Fagerli
_____
Disciplinary signature

2

Lars-Anders Breivik
_____
Responsible signature

1 Summary

This report contains estimates of atmospheric deposition of major inorganic compounds in Norway for the period 2017 to 2021 using two different methods: 1) from measurements of air and precipitation chemistry combined with spatial statistical fitting and 2) combining atmospheric chemical dispersion models with observations to infer pollutant deposition, so-called data fusion.

The traditional method, based on observations and statistical interpolation, has limitations in the spatial representativeness with sufficient number of sites and in the simplification of the dry deposition calculation, while the chemical transport model is dependent on good emission data as well as uncertainties in the meteorology and parameterisation of the model.

There is a very clear spatial gradient in the atmospheric deposition, seen by both methods, with the highest deposition loads in the south and south-west. This is due to the different level of precipitation amount in Norway, which is highest on the west coast, combined with highest contribution of long range transported air pollution from the continent to southern Norway. The wet deposition is the most important factor for the total deposition of inorganic compounds. In the areas with the highest total deposition, wet deposition contributes with 80-90% depending on compounds and method.

The data fusion method has improved the spatial information of the deposition pattern, and it likely gives more realistic spatial gradients of deposition than the observational based method. The combined method generally gives a lower deposition than the observational method, especially for nitrogen, however it produces higher estimates than implied by just the atmospheric chemical dispersion model.

Comparing the results for the observation based method with the previous period 2016-2021 estimated using the same approach, there is a decrease in the total sulfur and nitrogen deposition in Norway of 17% and 13% respectively. Since 1990, the deposition has decreased 74%, 25% and 20% for sulfur, oxidised- and reduced nitrogen, respectively.

Contents

2 Introduction

Atmospheric deposition of sulfur and nitrogen have harmful effects on ecosystems by causing acidification and eutrophication. The magnitude of deposition necessary for observing effects depends on the sensitivity of the different ecosystem. The limit of acceptable level of pollution is defined under the concept of critical load. This is an estimate of how much nature can receive from a pollutant without causing damage. The critical load concept forms the basis of several of the emission reduction protocols signed under the UN-ECE Convention on Long-Range Transboundary Air Pollution (LRTAP).

In order to evaluate the exceedance of critical loads to the ecosystems, quantified atmospheric input to the system is essential. There are three different approaches for calculating the atmospheric deposition over a larger region: 1) from measurements of air and precipitation chemistry combined with spatial modeling 2) from atmospheric chemical dispersion models using emission data, meteorological data and parameters describing transformation and removal processes or 3) combine observations and atmospheric model calculations, often called data assimilation or data-model fusion. In addition one can use throughfall measurements to estimate especially sulfur deposition. For modeling nitrogen deposition, there are many examples of statistical methods employed in the literature (*Schwede et al.*, 2011; *Schwede and Lear*, 2014; *Schwede et al.*, 2018, 2023; *Walker et al.*, 2020; *Wu et al.*, 2018; *Fu et al.*, 2022).

The atmospheric deposition estimates have in Norway historically been done using method 1) and have been reported every five years starting with the period 1978-1982 (*Pedersen et al.*, 1990; *Tørseth and Pedersen*, 1994; *Tørseth and Semb*, 1999; *Hole and Tørseth*, 2002; *Aas et al.*, 2007, 2012, 2017) There are two main limitations with this traditional observational based method. Firstly, at the Norwegian mainland, there are currently 13 regional sites with precipitation chemistry and only 4 with gas and aerosols measurements. Thus, there are large areas of Norway where these sites are not necessarily representative, and the uncertainty in the interpolation between these sites is large. Secondly, the dry deposition is not measured directly and it is necessary to estimate the deposition velocities based on literature values combined with information on climatic conditions and ground cover. These are very crude estimates, both spatially and temporally and do not take into account the interaction between species, i.e. co-deposition.

Atmospheric chemical transport models (CTMs) usually have a much higher spatial and temporal coverage and can potentially fill the gaps and limitations of the observational based method. In this report the CTM developed by the Norwegian Meteorological Institute (MET) under the Co-operative programme for monitoring and evaluation of long-range transmissions of air pollutants in Europe (EMEP) (*Simpson et al.*, 2012, 2022, and refs therein), which for Norway is with a finer resolution of 2.5km grids, EMEP4NO (*Denby et al.*, 2020; *Mu et al.*, 2022), is used in combination with observations to infer pollutant deposition through a data fusion.

Data fusion is the process of combining multiple sources of data to produce more accurate information about the process generating those data. Techniques have been successfully applied in various fields such as disease mapping, ecology, and air pollution. In this work, we seek to combine data sources with different levels of spatial support to infer the underlying spatial distribution of sulfur and nitrogen deposition. The model-measurement combined method was implemented in the previous estimates for 2012-2016 (*Aas et al.*, 2017). The method for fusing observations with model is developed for the period presented in this report: 2017-2021.

3 Methods

3.1 Observations

In the traditional observational based method, as well as for the fusion method, the measurements of sulfur and nitrogen components are from the national monitoring program in Norway (*Aas et al.*, 2022). One site (Osen) is from the ICP Forest program (*Timmermann et al.*, 2023). The sites are located in rural areas and are believed to generally give good estimates of long range transported pollutants. There are 15 sites with precipitation chemistry data in Norway and 4 sites with measurements in air and aerosols. In addition, concentrations in precipitation and air from neighbouring sites in Sweden and Finland have been used. All the data are available from the EBAS database infrastructure (*EBAS*, 2022) and the methods are described in *Aas et al.* (2022). The fusion has only been done with sulfate, nitrate and ammonium data from precipitation measurements.

At two of the sites (Kårvatn and Tustervatn) the ammonia concentrations are unrepresentative as they are influenced by nearby agricultural activities. The ammonium values (both in precipitation and in air) do not seem to be influenced significantly from these local sources, thus representative for long-range transported air. To have an estimate of the ammonia concentration at Kårvatn and Tustervatn, the ammonia concentration from Hurdal has been used as an estimate of the regional background concentration for these sites. For the observational based method, the sites very close to Russia (Svanvik and Karpbukt) have not been used due to influence from Nikel. Finnish and Swedish sites very far from the Norwegian border are also not used. The reason is that the kriging techniques will potentially give unrealistic high influence from sites which are not representative for Norwegian background concentrations and depositions. Table S1 gives an overview of which sites have been included in the two different methods.

The precipitation amount used for the calculations of wet deposition is taken from the MET Nordic dataset (*MET*, 2022), given on a $1 \times 1\,\mathrm{km}^2$ grid resolution. For the fusion method the precipitation has been interpolated to the EMEP $2.5 \times 2.5\,\mathrm{km}^2$ grid. The precipitation amount is aggregated to make annual deposition fields. These annual precipitation amount are shown in Figure S8 in the supplementary material.

Table 1: Deposition velocities (cm/s) for different inorganic compounds applied to the different landscape types and seasons.

| Compound | Land use classification | | | |
| | Forest | | Other | |
	Summer	Winter	Summer	Winter
SO_2	0.8	0.1	0.4	0.02
nss SO_4, sum (NH_3 + NH_4)	0.4	0.4	0.2	0.1
NO_2	0.4	0.02	0.2	0.02
sum (HNO_3 + NO_3)	2.0	2.0	1.0	0.25

3.2 Measurement based deposition

3.2.1 Estimating wet- and dry deposition

Wet deposition is obtained from the measured precipitation amounts in $1 \times 1\,\mathrm{km}^2$ resolution multiplied with the kriged $50 \times 50\,\mathrm{km}^2$ concentration field (see Section 3.2.2). This procedure does not include deposition by fog or dew, since the usual precipitation samplers generally collects no precipitation sample from such events.

For dry deposition, the measured concentrations in ambient air have been combined with seasonal deposition velocities for the different compounds. The various dry deposition processes and deposition rates are taken from the literature (e.g. *Fowler et al.*, 2009), and presented in Table 1. Discussion of the deposition velocities chosen for this study is presented in earlier reports i.e. by *Aas et al.* (2012). An important note is that the same procedure and deposition velocities have been used for all the periods since 1978-1982. However, it is recognized that for the latter decades there is a significant change in the atmospheric composition due to the large reductions in sulfur dioxide emissions, causing possible changes in the dry deposition velocities (*Aas et al.*, 2021).

3.2.2 Kriging station data

The interpolation of the concentrations in precipitation and air from fixed sites to a regular grid is done by kriging, a statistical method used to estimate values from neighbouring measurements. The method was originally developed for geostatistical purposes, often focused on mining operations (*Matheron*, 1963; *Journel and*

Huijbregts, 1981), but has since been used in connection with environmental studies for decades, e.g. on long range transported air pollutants (*Schaug et al.*, 1993).

The interpolations using this method in this work are performed using ordinary linear kriging. The kriging weights are computed from a variogram, which measures the degree of correlation among sample values in the area as a function of distance and direction of samples. A grid size of ca. $50 \times 50\,\text{km}^2$ (the old EMEP grid) has been applied. We use the R programming language and the `gstat` package (*Pebesma et al.*, 2015; *Gräler et al.*, 2016) for kriging and `autofitVariogram` from the automatic interpolation package `automap` (*Hiemstra et al.*, 2009). There are several parameters that control the fit of the variogram model and some of these can be constrained. In the `autofitVariogram` function users can fix the three variogram parameters: nugget, sill and range to a certain value as well as the covariance model used. We constrain the both the nugget (representing small-scale variability of the data), the range (the distance after which data are no longer correlated) and a Matérn covariance model based on Stein's parameterization (*Stein*, 1999). The nugget is set to 0 while the range to 5, equating to about 250 km ($50 \times 50\,\text{km}^2$ grid), which is reasonable considering the potential for long range transport of these pollutants. These covariance function parameters are selected on the basis of *a priori* knowledge rather than estimated (e.g., through maximum likelihood) due to the relatively small number of observations potentially leading to unstable estimates.

Seasonal averages of the mean airborne concentrations during winter (Jan. - Apr., Nov. - Dec.) and summer (May - Oct.) are calculated for SO_2, non-sea-salt (nss) SO_4, NO_2, NH_4^+, $NO_4^- + HNO_3$, and $NH_4^+ + NH_3$ for the four Norwegian sites combined with the Nordic measurements. These average contractions are interpolated to a $50 \times 50\,\text{km}^2$ grid using the kriging technique to obtain values for the individual grid cells. The dry deposition is estimated from the concentration fields and assessed dry deposition velocities for the two seasons, respectively. The dry deposition estimate is given for two land type categories; productive forests and other land use (e.g. unproductive land, rocks, agricultural land). When estimating the grid cell average, dry deposition is weighted on the distribution of land use types in the individual grid cells. The applied statistics on percentage productive forest in each cell is shown in Figure S1 in the Supplementary material.

3.3 Fusion of EMEP model output and station data

We also model wet depositions for 2017-2019 via a fusion framework proposed by *Moraga et al.* (2017), combining EMEP model data and observations from stations. This method combines data sourced with different levels of support (i.e., areal and point data) from which the spatial distribution of the underlying field is inferred using a Stochastic Partial Differential Equation (SPDE) and Integrated Nested Laplacian Approximation (INLA) approach (*Lindgren et al.*, 2011).

Henceforth, the spatial domain for the data fusion is taken to be

$$\mathcal{D} := [-3.25520°\text{W}, \, 33.924473°\text{W}] \times [56.58438°\text{N}, \, 72.11648°\text{N}].$$

The two data sources available are the EMEP model output, available at a $2.5 \times 2.5 \, \text{km}^2$ spatial resolution, and station data as outlined in Table S1. For different chemical species and different time frames, different numbers of stations are available. Throughout, we use only station data with at least 75% temporal coverage. Two-thousand EMEP points are sampled for each modeling scenario from the domain. The motivation for this is two-fold: 1) to reduce the computational burden, and 2) to prevent over fitting to the EMEP model output. The relatively high number of points and larger spatial support of the EMEP model output can have the adverse effect of influencing the fusion technique in a manner that relies too heavily on the EMEP model output, and does not allow for longer range effects of the station data to be observed in the fused field. Through experimentation, we find that sampling two-thousand EMEP point uniformly across the domain ensure a good balance of ability to model spatial structure at a relevant resolution, allowing enough distance between EMEP points to allow station data to exert some influence, and computational speed.

Our modeling strategy is to apply the fusion to concentrations in precipitation, and then multiply by the precipitation field in order to achieve the final wet deposition. This is preferable because the concentration in precipitation fields are generally smoother than the wet deposition fields. Additionally, we are able to incorporate the highest quality precipitation data available in the final step to model the wet deposition.

For example, at a point in space $\mathbf{s}$, the wet deposition of SOx is modeled by

$$WDEP\_\text{SOx}(\mathbf{s}) = CIP\_\text{SOx}(\mathbf{s}) \times Precip(\mathbf{s}),$$

where $CIP\_SOx(\mathbf{s})$ and $Precip(\mathbf{s})$ are the concentration in precipitation and precipitation, respectively. Therefore, the fusion approach subsequently described is applied to the concentration in precipitation fields, and then multiplied by a precipitation field to obtain the final wet deposition fields. The spatial statistical fusion framework assumes that the underlying field can be written in terms of the standard spatial model, where realizations z are written in terms of the additive model

$$z(\mathbf{s}) = \mu(\mathbf{s}) + y(\mathbf{s}) + \varepsilon(\mathbf{s}), \tag{1}$$

where $\mu(\mathbf{s})$ is a deterministic mean function, $y(\mathbf{s})$ is a stochastic process, and $\varepsilon(\mathbf{s})$ is an error term. The stochastic process in this case is taken to be a Gaussian process. The error term of Equation (1), ε, considered to be measurement error or small-scale variability, is often assumed to follow a mean-zero normal distribution with variance τ^2.

First the mean function μ must be estimated and removed in order to apply the fusion technique on the stochastic process y. To model the mean, we use functionality from the R package `LatticeKrig` (*Nychka et al.*, 2019), placing fifty-three compactly supported Wendland basis functions over the domain. Basis functions are placed according to an icosahedral knot-placement strategy to ensure approximately equal spacing across the domain. A Lasso regression model is then fit with these basis functions to the sampled EMEP model output and station data where the penalization parameter is chosen by 10-fold cross-validation. Weights are applied to the station data in the estimation of μ such that observations at stations have three-times the weight compared to the EMEP model output. No additional weighting is applied to the EMEP model output at this stage. This three-times weighting in the mean function was determined through consultation with domain experts, in which a survey found that three-to six times more weight should be applied to observations at stations than EMEP model output.

Once both data sources have been detrended, the geostatistical fusion model proposed by *Moraga et al.* (2017) is applied the residual fields, making use to the R package `inla` (*Lindgren and Rue*, 2015). This approach takes into account the different levels of support from both the EMEP model output and the station data. An exponential covariance function is used in each modeling setup. Through experimentation, we determine a weighting scheme which weights EMEP model output at station data as approximately equivalently represented in the likelihood yields
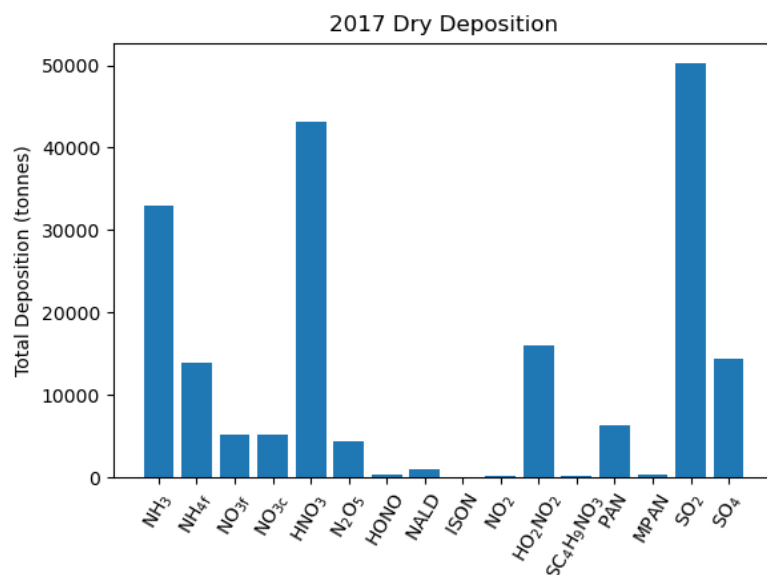
Figure 2: Contributions by species to dry deposition over the EMEP4NO domain.

good results.

Figure 2 presents chemical species' dry deposition contributions in 2017. The main contributor to dry deposition of reduced nitrogen is ammonia, but with substantial contribution of ammonium. For oxidized nitrogen, nitric acid is by far the most important contributor, and for oxidized sulphur dry deposition from both sulphur dioxide and sulphate contribute. For these key chemical contributors, there is relatively little available station data and thus we have at present chosen not to apply the fusion techniques for dry deposition. Moreover, dry deposition contributes relatively little in terms of total deposition in Norway. Consequently, to model dry deposition, just the EMEP model output is used, and no further modifications are made to the dry deposition estimates.

3.4 The EMEP MSC-W chemical transport model

The EMEP MSC-W model (*Simpson et al.*, 2012, 2022), a regional 3-D chemical transport model, is used in this study. The model version is the same as the version used by the EMEP Status Report 1/2022 (*Fagerli et al.*, 2022). There are two nested domains: the outer domain covering Europe (EMEP4EU) provides the boundary and initial conditions for the inner domain covering Norway (EMEP4NO). Therefore, the analysis is only based on the EMEP4NO outputs. The EMEP model has been

run for 5 years from 2017 to 2021, with the following setups:

3.4.1 EMEP4EU

- Meteorology: The meteorological data is extracted from the Integrated Forecast System (IFS) model of the European Centre for MediumRange Weather Forecasts (ECMWF), then is interpolated into a horizontal resolution of $0.1° \times 0.1°$ and 34 vertical layers. Version IFS Cycle 46r1 is used for 2019-2021, and version IFS Cycle 40r1 for 2017-2018.

- Domain: $[−29.95°\text{W}, 39.95°\text{W}] \times [34.95°\text{N}, 72.95°\text{N}]$, the standard EMEP01 domain.

- Emissions: The most recent emissions per country provided by the EMEP Centre on Emission Inventories and Projections (CEIP, `www.ceip.at`) in June 2022 for the years 2017 to 2020. Year 2021 uses the same emissions as 2020. The resolution is $0.1° \times 0.1°$. The GNFR sector C (small-scale combustion) of PMs are replaced by an updated TNO Ref2 (version v2.1) emission data considering condensable components. This combined emission data set has been used in the EMEP Status Report 1/2022.

3.4.2 EMEP4NO

- Meteorology: AROME meteorology at the resolution of 2.5 km. Since a good simulation of precipitation is crucial for wet deposition study, we have tested several precipitation data sets.

- Domain: $[−3.26°\text{W}, 33.92°\text{W}] \times [56.58°\text{N}, 72.12°\text{N}]$, the standard EMEP4NO domain.

- Emissions: Within Norway, we use the high-resolution Norwegian emissions for the traffic and the residential sectors prepared from local emission data. For other emission sectors in Norway and all sectors outside of Norway, we use the same emissions as those in the EMEP4EU run.

1. The original 2D precipitation from AROME meteorology.

2. The 2D precipitation from the Nordic reanalysis data set, which has assimilated surface precipitation observations. The resolution is 1 km, but is interpolated into 2.5 km resolution.

3. The 3D precipitations with 20 vertical layers. The 3D precipitations are reconstructed based on the accumulated surface precipitations and the mass fraction of water in air. The water in air is obtained from the AROME metdata as the sum of rain, graupel and snow. Since we need the accumulated 3D precipitations and the water amounts are given as instantaneous values, some transformations are first required: The water values are smoothed in space, and the average value between two time steps is then taken. The resulting 3D fields are then scaled according to the surface precipitations, so that at the lowest level, the 2D and 3D precipitations are equal. Further we require that 3D precipitations cannot increase with increasing height in the same vertical column.

4. Same as (3) but with a newly developed photolysis scheme for the EMEP model - using the "CloudJ" system (*Prather*, 2015). The CloudJ scheme will be the default in future EMEP versions (*van Caspell, W.E. et al.*, 2023).

5. Same as (3) but with 21 vertical layers. The extra layer is implemented in the middle of the lowest layer.

3.5 Comprehensive model evaluation

A comprehensive model evaluation against the measurements is done by the AeroVal system[1]. Modeled air components and wet depositions are compared to the rural stations of the Air Quality e-Reporting (EEA-rural), as well as the EBAS database. We wish to find out which precipitation dataset is the best to use.

For this project, we want the modeled precipitation and wet depositions of sulfate (Wet SOx), ammonium (Wet NHx) and nitrate (Wet NOx) as accurately as possible. Figure S2 shows that the standard AROME meteorology ('2Dprecip') has in general the lowest normalized mean bias. The spacial and temporal correlations are both very high (Figure S3 and Figure S4). Other precipitation data set either has no

---

[1]`https://aeroval.met.no/`
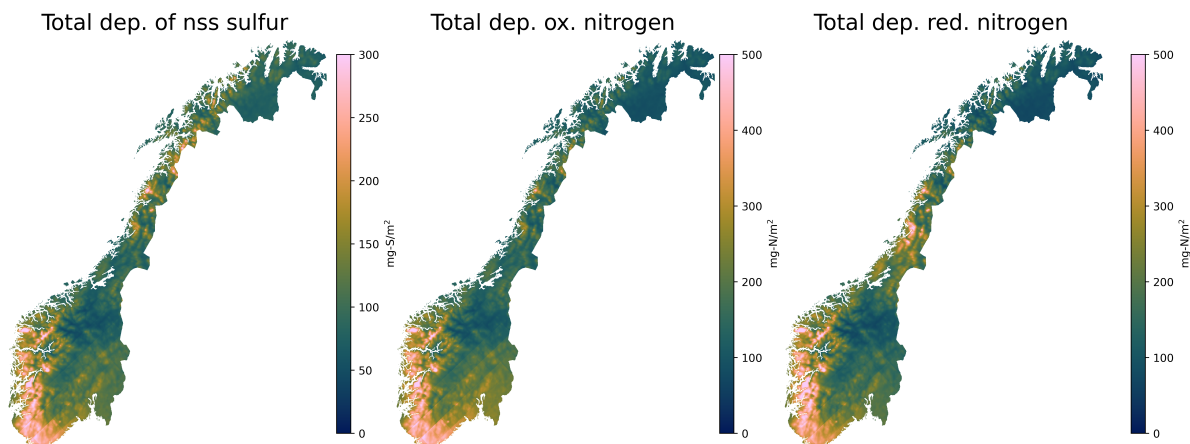
Figure 3: Total deposition of non sea salt sulfur, oxidized- and reduced nitrogen, annual mean averages for the period 2017-2021 from the observation-based method

obvious improvement or is even worse. Therefore, we decided to use the standard AROME meteorology to run the EMEP model in this project.

4 Results and discussions

4.1 Measurement based deposition estimates

Maps of total deposition of total non sea salt (nss) sulfur, oxidized- and reduced nitrogen estimated with the observational based method are shown in Figure 3. The total deposition of the non-sea-salt compounds was highest in the south-western part of Norway as a combination of relatively high concentrations and large precipitation amounts, whereas the lowest depositions were observed in the north and central Norway. The highest deposition of non-sea salt sulfur was around 300 mg mg S/m²/yr and around 500 mg N/m²/yr for both reduced- and oxidized nitrogen.

The wet deposition is the most important factor for deposition of inorganic compounds, illustrated in Figure 4, with 90% contribution to the total deposition for both sulfur and nitrogen in the areas with highest deposition loads. In areas with little precipitation the dry deposition is relatively more important, but still most areas are below 30% dry deposition. For the total deposition, the dry deposition contributes with 12%, 22% and 8% for sulfur, oxidized- and reduced nitrogen respectively.
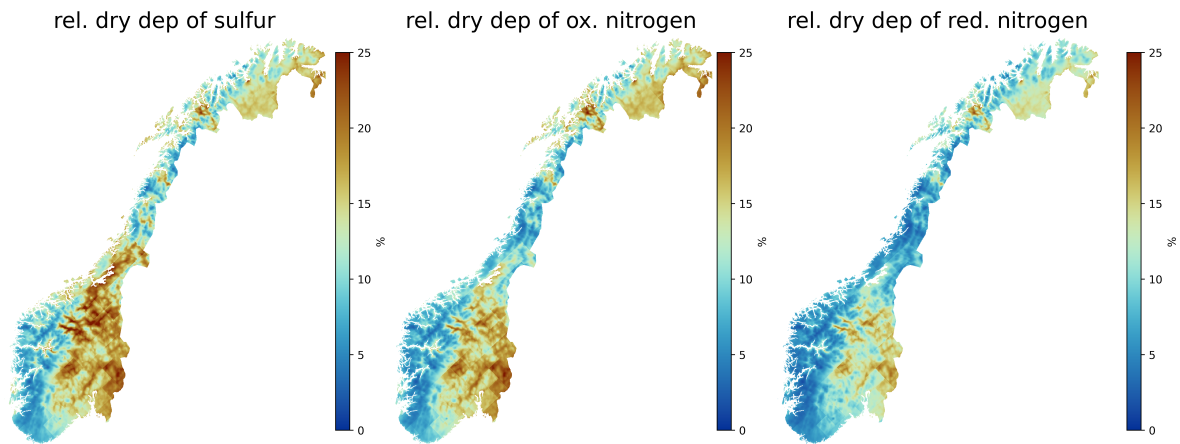
Figure 4: The relative contribution of dry deposition to the total deposition of non sea salt sulfur, oxidized- and reduced nitrogen. Aggregated to annual mean average for the period 2017-2021 from the observation-based method.

4.2 Deposition estimates based on fusion of model results and observations

The data fusion section described in Section 3.3 is applied to produce maps of wet deposition for SOx, NOx, and NHx in Norway. Figure S5 shows the EMEP output for these fields with observations at stations superimposed. Dry deposition fields are taken from the EMEP model, and summed with the associated wet deposition fields estimate the total deposition. Figure 6 presents the average wet and dry deposition from this method from 2017 to 2021. Figure 5 shows the constituent wet and dry depositions, respectively.

4.3 Differences between measurement and fusion-based estimates

Figure 7 shows the difference in total deposition between the measurement-based deposition estimates and the fusion-based estimates in terms of original units (mg S and mg $N/m^2/yr$) and percentages. There is a clear pattern with the fusion method giving higher deposition at the coast while the observational method are higher inland, especially in the mountainous area. This negative bias is a weakness of the kriging method, which moves the gradient away from the site. The EMEP model tends to give higher concentrations along the coast since the model assumes washout of the air pollution faster than the kriging method.

The fusion-based method has lower estimates of total deposition in Norway compared to the observational based method by 1%, 36% and 28% for sulfur, oxidized- and reduced nitrogen respectively, Table 2. This can partly be explained by the very different dry deposition rates used for nitrate, but could also be due to underestimation of NOx and NHx emissions. The EMEP model relies on these emission estimates, and so systematic underestimation in the EMEP fields will transfer over to the predictions produced by the fusion technique. On the other hand, the kriging-based technique could over estimate as a result of model misspecification (e.g., the chosen covariance function parameters and fixed intercept in the model).

The methods are comparable and resemble the same general pattern of deposition throughout the country with higher deposition closer to the main emission sources in Europe, but with some regional differences. The combined method has improved the spatial information of the deposition pattern and for wet deposition it probably gives more realistic deposition than the old observation method. For dry deposition there are quite large uncertainties in the estimated dry deposition velocities in both methods. Further, there are also quite large uncertainties in the observations as well as the reported emissions. The relatively few sites, especially for air components, makes it difficult to estimate the distance of influence of the measurements when adjusting the model results. Considering these uncertainties, there is higher confidence in the deposition estimates of sulfur than nitrogen.

4.4 Differences between EMEP and fusion-based estimates

Table 2 shows the total deposited pollutants for 2017-2021 as estimated by the EMEP model and the fusion technique. Compared to the EMEP model, the fu-
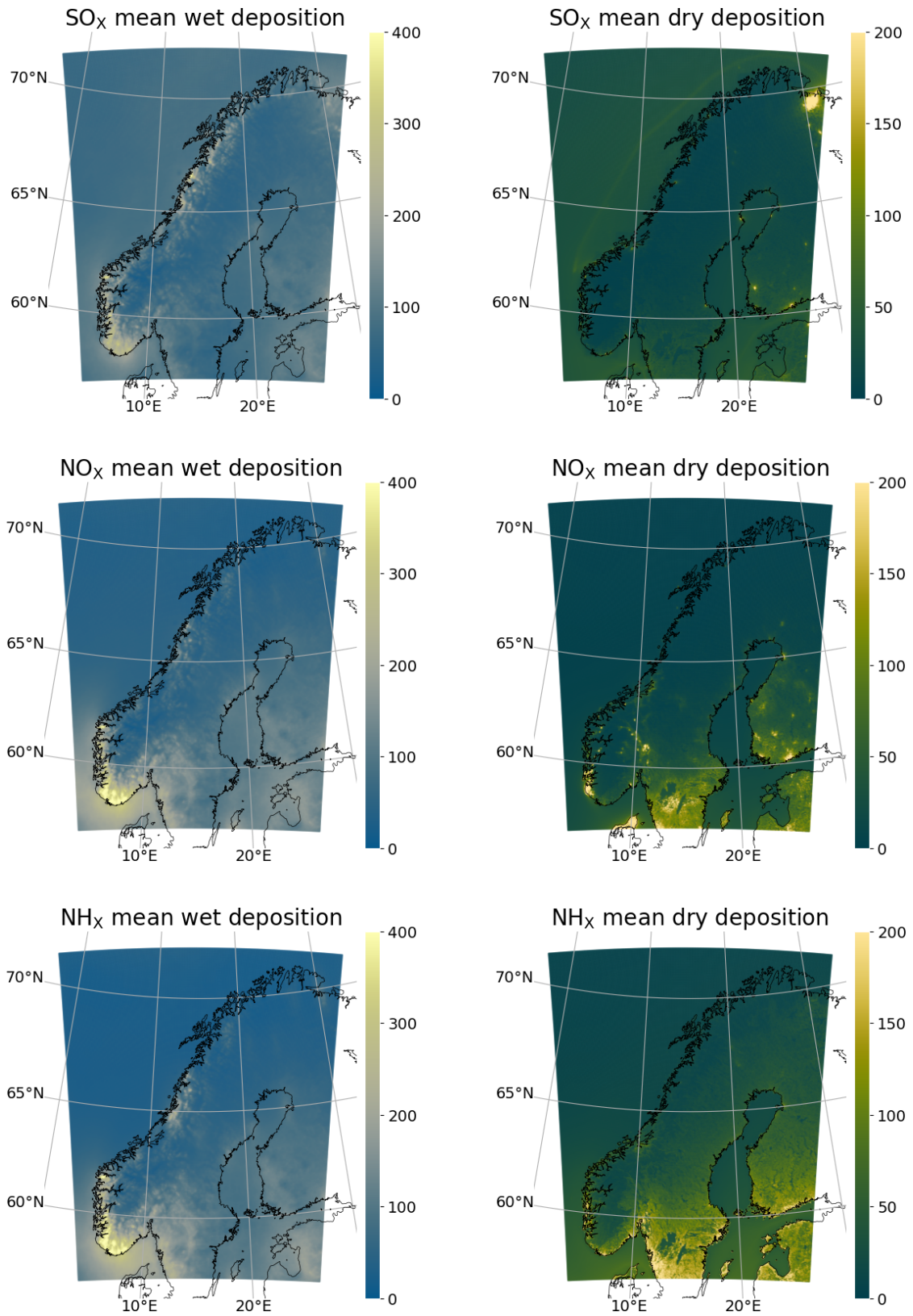
Figure 5: Average wet and dry deposition over 2017-2021 from the measurement-model fusion method in units of mg $S/m^2/yr$ and mg $N/m^2/yr$, respectively.
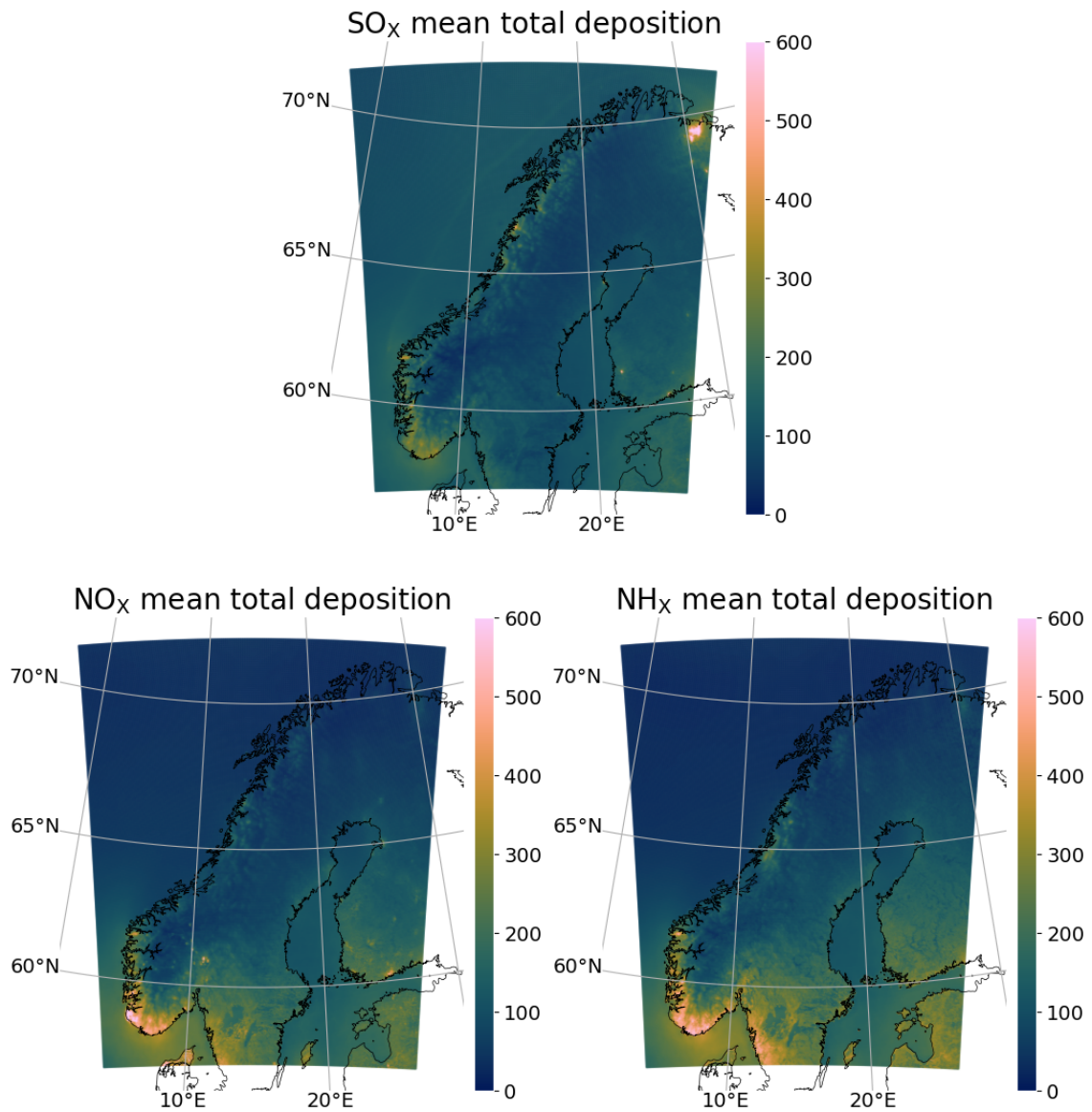
Figure 6: Average total deposition 2017-2021 from the measurement-model fusion method in units of mg S/m^2/yr and mg N/m^2/yr, respectively.

sion technique predicts about 10%, 31%, and 55% more total deposition for sulfur, oxidized- and reduced nitrogen respectively. Figure S7 presents the difference between the EMEP output and the fused field. Here we can see that in areas where observations and EMEP differ the fused field is pulled in the direction of the observations. Differences present may also result from the differing precipitation fields used. Whereas EMEP has its own internal precipitation scheme, we use the Nordic precipitation data set provided by MET (*MET*, 2022) and shown in Figure S8, which accounts for some other differences between these fields. In general, however, where observations are not available, the fused fields and EMEP output are in agreement.
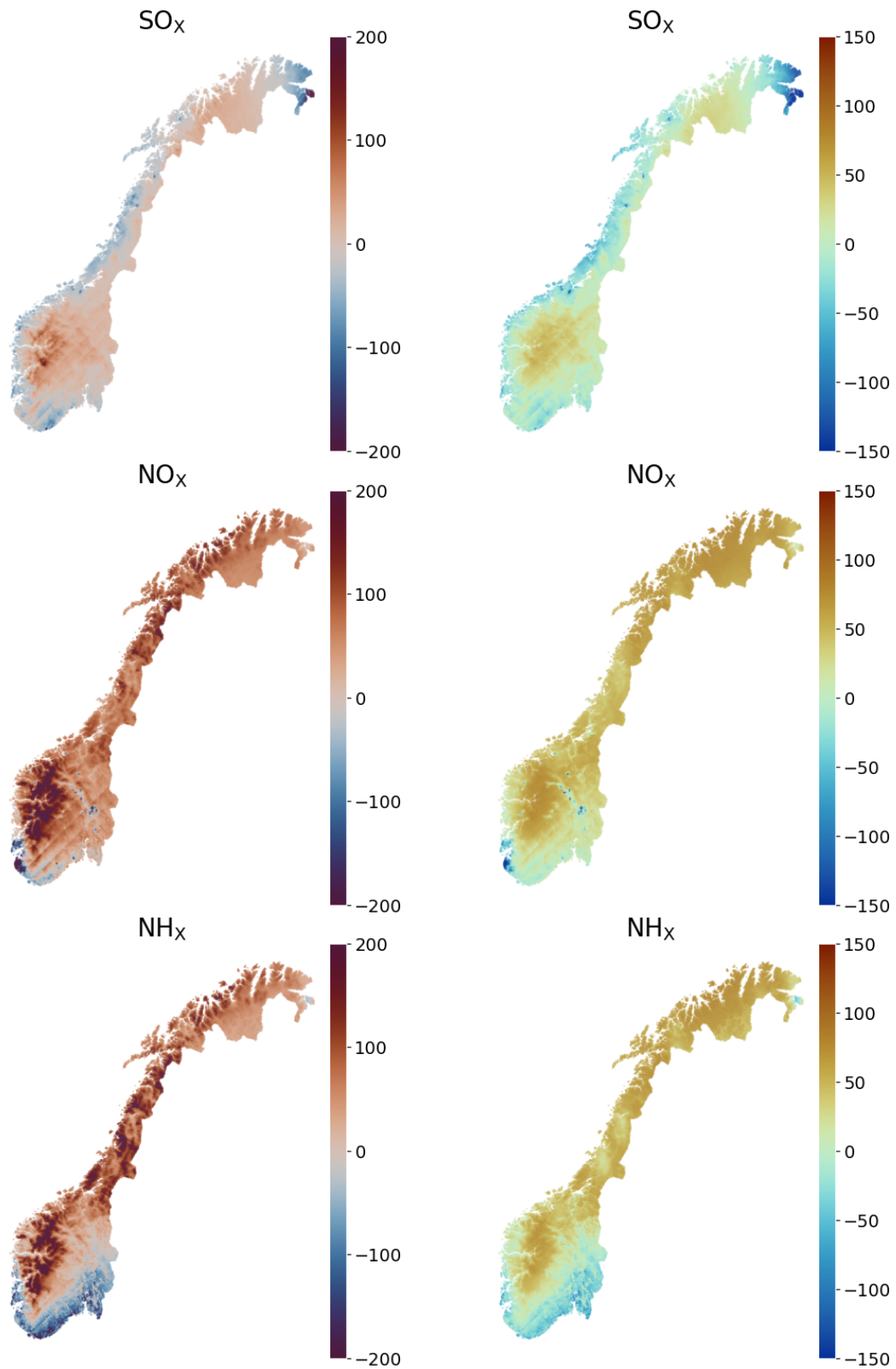
Figure 7: Average difference in units of mg S/m²/yr and mg N/m²/yr (left column) and percentage difference (right column) between methods over 2017-2021, calculated as observational method minus the fusion method

Table 2: Total depositions in tonnes over Norway accumulated over 2017 - 2021 as determined by EMEP and the two methods.

	SOx	NOx	NHx
EMEP Model	163 859	142 184	93 622
Observation-based	182 256	291 181	289 504
Data Fusion	180 652	186 632	209 696

4.5 Trends in deposition of sulphur and nitrogen, 1978-2021

It is not possible to do any trend assessment using the results from fusion since this method has not been used for other periods. With the observational based kriging method it is possible to estimate trends in deposition from the first assessment in 1978-1982. Trend in total sulfur depositions are shown in Figure 8 and total nitrogen in Figure 9. The total deposition to Norway compared to the European sulfur emissions are shown in Figure 10. The emissions are the sum of emissions from the EMEP Parties reported to CEIP (`https://www.ceip.at`), excluding the emissions in Caucasus and Central Asia.

There is a significant decreasing trend in sulfur deposition since 1980, a decrease of more than 80% of the total amount deposited in Norway. The trend in sulfur deposition is very well correlated with the total emission trends in Europe, see Table 3 and are in line with observations for the rest of Europe (*Aas et al.*, 2021; *Colette et al.*, 2021).

For nitrogen there is also a downward trend, though less than for sulfur and more for oxidised nitrogen than for reduced nitrogen, Table 3. Since 1990 the reductions in total NOx deposition has been 25% while for NHx 20%. The decline in emissions of NOx is higher than the observed trend in deposition, while the opposite is the case for NHx. The reason can be that the reported trend in emissions of NOx are too optimistic (*Colette et al.*, 2021) while for ammonium the trends is related to the trend in sulfate. There is less SO_2 available to associate with NH_3, thus there is less ammonium sulfate available to be long range transported to Norway (*Aas et al.*, 2021).

In the review of the Gothenburg Protocol an assessment of the trends in air

22
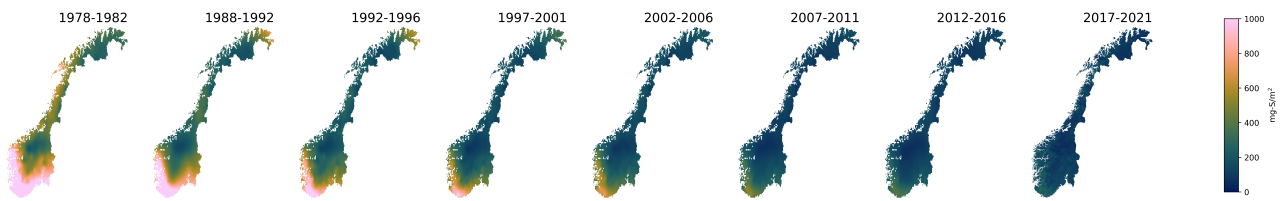
Figure 8: Trends in total deposition of non sea salt (nss) sulfur
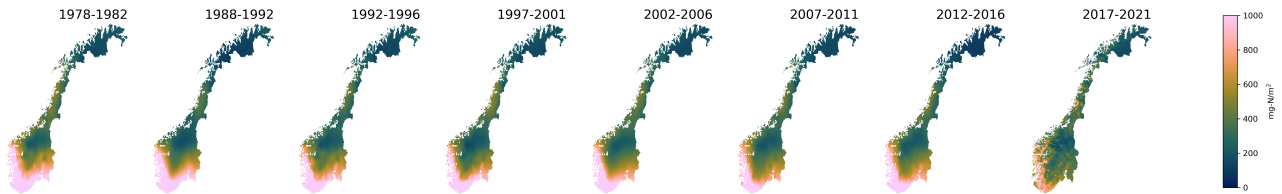
Figure 9: Trends in total deposition of nitrogen

Table 3: Relative change in total deposition in Norway compared to total change in emissions in EMEP, excluding emissions from Caucasus and Central Asia.

	SOx		Nox		NHx	
	obs.	emissions	obs.	emissions	obs.	emissions
change from 1980	-81%	-89%	-27%	-52%	-34%	-23%
change from 1990	-74%	-78%	-25%	-43%	-20%	-24%
change from 2000	-55%	-69%	-16%	-37%	-21%	-27%
change from 2015	-17%	-39%	-10%	-13%	-17%	-2%
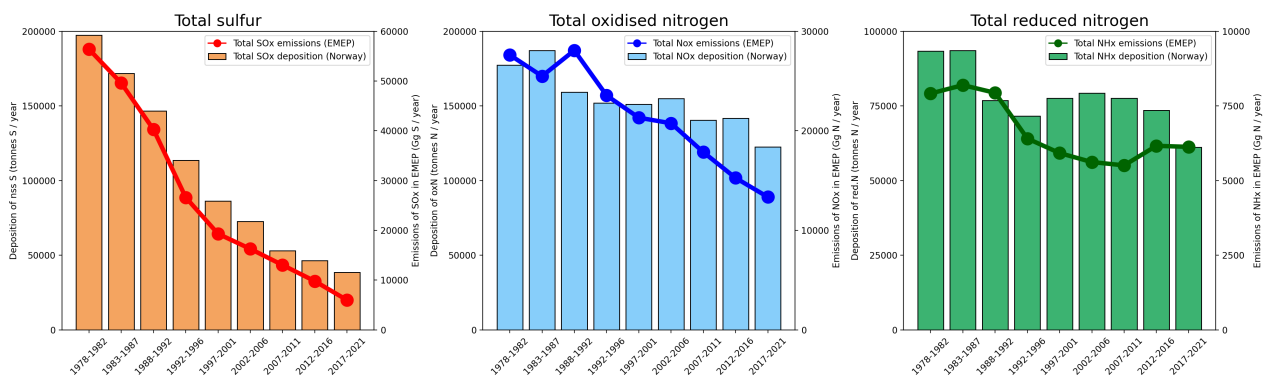
Figure 10: Total deposition of sulfur and nitrogen (tonnes/year in Norway (tonnes/year) compared with emissions in Europe (Gg/year).

23

pollution in Europe for the period 2000–2019 based on long term observational data from the EMEP network as well as EMEP MSC-W model calculations were performed (*Aas et al.*, 2022). To make the data and the results more easily accessible, the trend work has been made available through a web interface. This interface also allows country representatives to understand, interpret and analyze data for their own area more easily. The EMEP Trend Interface is available on the AeroVal web-page (`https://aeroval.met.no/evaluation.php?project=emep-trends`). Observed and modelled trends were processed with the Python package `pyaerocom`[2] for the period 2000–2019. The trends in observed and modelled wet deposition of sulfur and nitrogen from this web interface is shown in Figure 11. The trends in model and observations are similar except that for oxidised nitrogen the modelled trends show somewhat higher reductions than observations. This is probably due to too optimistic reporting in the emissions of NOx.

5 Conclusions

We have presented and studied two methods for estimating nitrogen and sulfur depositions in Norway for 2017-2021. Both techniques take the approach of modeling through concentration in precipitation, and then introducing the highest quality available precipitation data available at the final stage to produce deposition maps. The techniques differ in sophistication as well as the implied deposition fields they produce. Differences in the results produce by the two methods can occur for several reasons.

The purely observation-based technique uses classical statistical tools to infer concentration in precipitation at stations by fitting a spatial process to them. The intercept is set to zero while the covariance function parameters are chosen based on domain expertise about, among other factors, the expected long-range transportation distances of these chemical species. This approach relies on a relatively small number of observations to infer the spatial distribution of the concentration in precipitation for each chemical species. The small number of observations can limit reliable parameter estimation, and so parameters needed to fit the model are be chosen on the basis of *a priori* information. Imposing these parameter choices, in conjunction with the assumption of a constant mean throughout, introduces some

---

[2]`https://github.com/metno/pyaerocom`
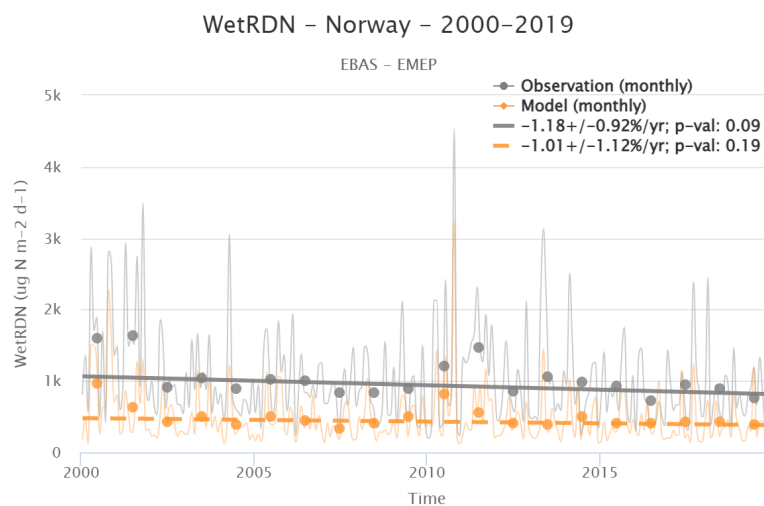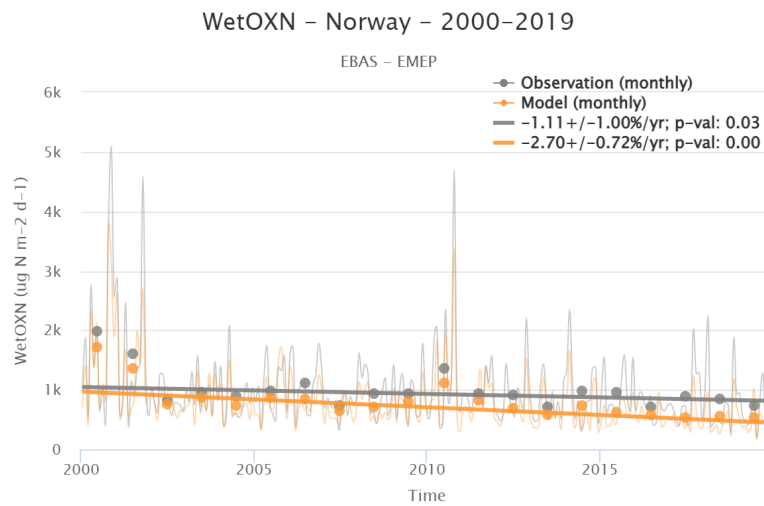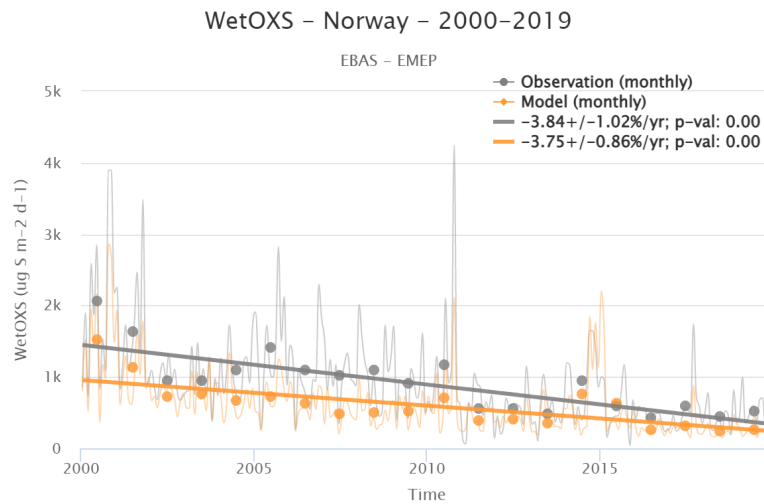
Figure 11: Trends in wet deposition of sulfur (WetOXS), oxidised- and reduced nitrogen (WetOXN and WetRDN) in EMEP observations and EMEP/MSC-W model, 2000-2019

inflexibility into the model and may lead to deposition estimates which are less representative of reality.

Our new approach uses a data fusion model proposed by *Moraga et al.* (2017), combining EMEP model output with station data, alongside more sophisticated spatial modeling techniques, in order to compensate for the relatively small number of available station data. This approach allows combining these two different data sources, accounting for their different levels of support, and weighting them differently based on prior knowledge. The increased the amount of data available in this second approach facilitates more reliable statistical estimation of modeling parameters through gradient descent methods. These data-driven model parameter estimates result in what we expect to be more representative deposition maps. Modeling choices in the fusion technique which contribute to the differences observed between the methods include the number of points sampled, the sampling locations, the weighting setup chosen, and the choice mean function. While we expect the fusion technique produces more realistic deposition maps, the fusion technique could be improved upon in future work, in which additional techniques for debiasing, or "calibration", of the EMEP model are further examined and employed.

Both techniques are consistent in that they produce deposition maps which lead to the largest deposition in southern and south-western Norway. The primary reason for this is that wet deposition contributes the majority of deposition of sulfur and nitrogen in Norway. These areas are consequently expected to have the largest deposition due to contributions from long range transported air pollution from continental Europe being felt most significantly in the southern part of the country and the increased rainfall in the western part of the country.

The data fusion based method is not compared to previous periods as it was not previously implemented. The observation-based method which has been implemented in years prior produces maps which indicate a decrease in the trend of both sulfur and nitrogen in the period 2017-2021 compared to years past. This is in line with the reported emission trends in Europe and the trends in the EMEP model results for Norway.

Acknowledgements

References

Aas, W., J. Schaug, and J. Hanssen (2007), Field intercomparison of main components in air in emep, *Water, Air, & Soil Pollution: Focus*, *7*(1), 25–31.

Aas, W., A.-G. Hjellbrekke, L. Hole, and Tørseth (2012), Deposition of major inorganic compounds in norway 2007-2011, *Tech. Rep. NILU OR 41/2012*, Norwegian Institute for Air Research, Kjeller, Norway.

Aas, W., A.-G. Hjellbrekke, H. Fagerli, and A. Benedictow (2017), Deposition of major inorganic compounds in norway 2012-2016, *Tech. Rep. NILU OR 41/2017*, Norwegian Institute for Air Research, Kjeller, Norway.

Aas, W., H. Fagerli, K. Yttri, S. Tsyro, S. Solberg, D. Simpson, J. Gliß, A. Mortier, E. G. Wærsted, H. Brenna, A.-G. Hjellbrekke, J. Griesfeller, A. Nyíri, and T. Gauss M, Scheuschner (2021), Trends in observations and emep msc-w model calculations 2000-2019, in *Transboundary particulate matter, photo-oxidants,acidifying and eutrophying components (EMEP Status Report 1/2021)*, pp. 59–106, The Norwegian Meteorological Institute, Oslo, Norway.

Aas, W., T. F. Berglen, S. Eckhardt, M. Fiebig, S. Solberg, and K. Yttri (2022), Monitoring of long-range transported air pollutants in norway, annual report 2021, *Tech. Rep. NILU OR 18/2022, M-2303*, Norwegian Institute for Air Research, Kjeller, Norway.

Colette, A., S. Solberg, W. Aas, , and S.-E. Walker (2021), Understanding air quality trends in europe, focus on the relative contribution of changes in emission of activity sectors, natural fraction and meteorological variability, *Tech. Rep. EIONET report ETC/ATNI 2020/8*, European Topic Centre on Air pollution, transport, noise and industrial pollution, Kjeller, Norway.

Denby, B. R., M. Gauss, P. Wind, Q. Mu, E. Grøtting Wærsted, H. Fagerli, A. Valdebenito, and H. Klein (2020), Description of the uEMEP_v5 downscaling approach for the EMEP MSC-W chemistry transport model, *Geoscientific Model Dev.*, *13*(12), 6303–6323, doi:10.5194/gmd-13-6303-2020.

EBAS (2022), Ebas data base infrastructure, `https://ebas.nilu.no/data-access/`, accessed: 2022-10-07.

Fagerli, H., A. Benedictow, B. Denby, M. Gauss, D. Heinesen, J. Jonson, K. Karlsen, H. Klein, A. Mortier, A. Segers, D. Simpson, S. Tsyro, P. Wind, W. Aas, A. Hjellbrekke, S. Solberg, S. Platt, K. Yttri, B. Matthews, S. Schindlbacher, B. Ullrich, Z. Klimont, T. Scheuschner, I. Fernandez, and J. Kuenen (2022), Transboundary particulate matter, photo-oxidants, acidifying and eutrophying, components. emep status report 1/2022, *Tech. rep.*, Meteorologisk institutt | Norwegian Meteorological Institute.

Fowler, D., K. Pilegaard, M. Sutton, P. Ambus, M. Raivonen, J. Duyzer, D. Simpson, H. Fagerli, S. Fuzzi, J. Schjoerring, C. Granier, A. Neftel, I. Isaksen, P. Laj, M. Maione, P. Monks, J. Burkhardt, U. Daemmgen, J. Neirynck, E. Personne, R. Wichink-Kruit, K. Butterbach-Bahl, C. Flechard, J. Tuovinen, M. Coyle, G. Gerosa, B. Loubet, N. Altimir, L. Gruenhage, C. Ammann, S. Cieslik, E. Paoletti, T. Mikkelsen, H. Ro-Poulsen, P. Cellier, J. Cape, L. Horváth, F. Loreto, Ü. Niinemets, P. Palmer, J. Rinne, P. Misztal, E. Nemitz, D. Nilsson, S. Pryor, M. Gallagher, T. Vesala, U. Skiba, N. Brüeggemann, S. Zechmeister-Boltenstern, J. Williams, C. O'Dowd, M. Facchini, G. de Leeuw, A. Flossman, N. Chaumerliac, and J. Erisman (2009), Atmospheric composition change: Ecosystems-atmosphere interactions, *Atmos. Environ.*, *43*, 5193–5267, doi:10.1016/j.atmosenv.2009.07.068.

Fu, J. S., G. R. Carmichael, F. Dentener, W. Aas, C. Andersson, L. A. Barrie, A. Cole, C. Galy-Lacaux, J. Geddes, S. Itahashi, M. Kanakidou, L. Labrador, F. Paulot, D. Schwede, J. Tan, and R. Vet (2022), Improving estimates of sulfur, nitrogen, and ozone total deposition through multi-model and measurement-model fusion approaches, *Environ. Sci. Technol.*, *56*(4), 2134–2142, doi:10.1021/acs.est.1c05929, pMID: 35081307.

Gräler, B., E. J. Pebesma, and G. B. Heuvelink (2016), Spatio-temporal interpolation using gstat., *R J.*, *8*(1), 204.

Hiemstra, P. H., E. J. Pebesma, C. J. Twenhöfel, and G. B. Heuvelink (2009), Real-time automatic interpolation of ambient gamma dose rates from the dutch radioactivity monitoring network, *Computers & Geosciences*, *35*(8), 1711–1721.

Hole, L., and Tørseth (2002), Deposition of major inorganic compounds in nor-

way 1978-1982 and 1997-2001: status and trends, *Tech. Rep. NILU OR 61/2002*, Norwegian Institute for Air Research, Kjeller, Norway.

Journel, A., and C. Huijbregts (1981), J.(1981) mining geostatistics.

Lindgren, F., and H. Rue (2015), Bayesian spatial modelling with r-inla, *Journal of statistical software*, *63*, 1–25.

Lindgren, F., H. Rue, and J. Lindström (2011), An explicit link between gaussian fields and gaussian markov random fields: the stochastic partial differential equation approach, *Journal of the Royal Statistical Society: Series B (Statistical Methodology)*, *73*(4), 423–498.

Matheron, G. (1963), Principles of geostatistics, *Economic geology*, *58*(8), 1246–1266.

MET (2022), Met nordic dataset, `https://github.com/metno/NWPdocs/wiki/MET-Nordic-dataset`, accessed: 2022-10-07.

Moraga, P., S. M. Cramb, K. L. Mengersen, and M. Pagano (2017), A geostatistical model for combined analysis of point-level and area-level data using inla and spde, *Spatial Statistics*, *21*, 27–41.

Mu, Q., B. R. Denby, E. G. Wærsted, and H. Fagerli (2022), Downscaling of air pollutants in Europe using uEMEP_v6, *Geoscientific Model Dev.*, *15*(2), 449–465, doi:10.5194/gmd-15-449-2022.

Nychka, D., D. Hammerling, S. Sain, N. Lenssen, and M. D. Nychka (2019), Package 'latticekrig'.

Pebesma, E., B. Graeler, and M. E. Pebesma (2015), Package 'gstat', *Comprehensive R Archive Network (CRAN)*, pp. 1–0.

Pedersen, U., S. Walker, and A. Kibsgaard (1990), Deposition mapping of sulphur and nitrogen compounds in norway., *Tech. Rep. NILU OR 28/90*, Norwegian Institute for Air Research, Kjeller, Norway.

Prather, M. J. (2015), Photolysis rates in correlated overlapping cloud fields: Cloud-j 7.3c, *Geoscientific Model Development*, *8*(8), 2587–2595, doi:10.5194/gmd-8-2587-2015.

Schaug, J., T. Iversen, and U. Pedersen (1993), Comparison of measurements and model results for airborne sulphur and nitrogen components with kriging, *Atmospheric Environment. Part A. General Topics*, *27*(6), 831–844.

Schwede, D., L. Zhang, R. Vet, and G. Lear (2011), An intercomparison of the deposition models used in the castnet and capmon networks, *Atmos. Environ.*, *45*(6), 1337–1346, doi:10.1016/j.atmosenv.2010.11.050.

Schwede, D. B., and G. G. Lear (2014), A novel hybrid approach for estimating total deposition in the united states, *Atmos. Environ.*, *92*, 207 – 220, doi:https://doi.org/10.1016/j.atmosenv.2014.04.008.

Schwede, D. B., D. Simpson, J. Tan, J. S. Fu, F. Dentener, E. Du, and W. deVries (2018), Spatial variation of modelled total, dry and wet nitrogen deposition to forests at global scale, *Environ. Poll.*, *243*, 1287 – 1301, doi:https://doi.org/10.1016/j.envpol.2018.09.084.

Schwede, D. B., D. Simpson, F. Dentener, E. Du, and W. de Vries (2023), Modelling nitrogen deposition in global forests, in *Atmospheric Nitrogen Deposition to Global Forests*, pp. XXXX, in press, Environmental Pollution Special Issue, Elsevier.

Simpson, D., A. Benedictow, H. Berge, R. Bergström, L. D. Emberson, H. Fagerli, C. R. Flechard, G. D. Hayman, M. Gauss, J. E. Jonson, M. E. Jenkin, A. Nyíri, C. Richter, V. S. Semeena, S. Tsyro, J.-P. Tuovinen, A. Valdebenito, and P. Wind (2012), The EMEP MSC-W chemical transport model – technical description, *Atmos. Chem. Physics*, *12*(16), 7825–7865, doi:10.5194/acp-12-7825-2012.

Simpson, D., I. Gonzalez Fernandez, A. Segers, S. Tsyro, A. Valdebento, and P. Wind (2022), Updates to the EMEP/MSC-W model, 2021–2022, in *Transboundary particulate matter, photo-oxidants, acidifying and eutrophying components. EMEP Status Report 1/2022*, pp. 133–146, The Norwegian Meteorological Institute, Oslo, Norway, available from www.emep.int.

Stein, M. L. (1999), *Interpolation of spatial data: some theory for kriging*, Springer Science & Business Media.

Timmermann, V., I. Børja, and N. e. a. Clarke (2023), Skogens helsetilstand i norge.

resultater fra skogskadeovervækingen i 2021, *Tech. Rep. NIBIO 39/2023*, NIBIO, Ås, Norway.

Tørseth, K., and U. Pedersen (1994), Deposition of sulphur and nitrogen compounds in norway 1988-1992, *Tech. Rep. NILU OR 16/94*, Norwegian Institute for Air Research, Kjeller, Norway.

Tørseth, K., and A. Semb (1999), Deposition of major inorganic compounds in norway 1992-1996, *Tech. Rep. NILU OR 67/97*, Norwegian Institute for Air Research, Kjeller, Norway.

van Caspell, W.E., et al. (2023), Updated photolysis rates in the emep msc-w chemical transport model using cloud-j v7.3e, *In preparation.*

Walker, J. T., G. Beachley, L. Zhang, K. B. Benedict, B. C. Sive, and D. B. Schwede (2020), A review of measurements of air-surface exchange of reactive nitrogen in natural ecosystems across north america, *Sci. of the Total Environ.*, *698*, 133,975, doi:https://doi.org/10.1016/j.scitotenv.2019.133975.

Wu, Z., D. B. Schwede, R. Vet, J. T. Walker, M. Shaw, R. Staebler, and L. Zhang (2018), Evaluation and Intercomparison of Five North American Dry Deposition Algorithms at a Mixed Forest Site, *Journal of Advances in Modeling Earth Systems*, *10*(7), 1571–1586, doi:https://doi.org/10.1029/2017MS001231.

Supplementary material

This supplementary provides extra information on wfrom which sites data has been used and additional figures of depostion for the individual years etc.

Table S1: The sites used in the observational based method and in the fusion

| | | | | SO$_4$, NH$_4$, NO$_3$ precipitation | | Air and aerosols obs. method | | |
Code	Station name	latitude	longitude	obs. method	fusion	SO$_2$, SO$_4$, NO$_3$,HNO$_3$,NH$_4$	NH$_3$	NO$_2$
FI0004R	Ähtäri	62.533	24.222		x			
FI0008R	Kevo	69.750	27.000	x	x			
FI0018R	Virolahti III	60.530	27.668		x			
FI0022R	Oulanka	66.320	29.402		x			
FI0036R	Pallas (Matorova)	68.000	24.237	x	x	x	x	x
FI0050R	Hyytiälä	61.850	24.283		x			
FI0053R	Hailuoto II	65.000	24.694		x			
FI0092R	Hietajärvi	63.167	30.717		x			
FI0093R	Kotinen	61.233	25.067		x			
NO0001-2R	Birkenes I og II	58.383	8.250	x	x	x	x	x
NO0015R	Tustervatn	65.833	13.917	x	x	x		x
NO0039R	Kårvatn	62.783	8.883	x	x	x		x
NO0047R	Svanvik	69.450	30.033		x			
NO0056R	Hurdal	60.372	11.078	x	x	x	x	x
NO0218R	Løken	59.805	11.461	x	x			
NO0236R	Treungen	59.017	8.517	x	x			
NO0237R	Vatnedalen	59.467	7.367	x	x			
NO0478R	Høylandet	64.647	12.312	x	x			
NO0554R	Haukeland	60.817	5.583	x	x			
NO0572R	Vikedal	59.537	5.972	x	x			
NO0655R	Nausta	61.577	5.898		x			
NO1041R	Osen (forest)	61.284	11.853	x	x			
NO1218R	Brekkebygda	60.300	9.733	x	x			
NO1241R	Karpbukt	69.667	30.367		x			
SE0005R	Bredkälen	63.850	15.333	x	x	x	x	x
SE0012R	Aspvreten	58.800	17.383	x	x			
SE0013R	Esrange	67.883	21.067	x	x			x
SE0014R	Råö	57.394	11.914	x	x	x	x	x
SE0020R	Hallahus	56.043	13.148	x	x			
SE0022R	Norunda Stenen	60.086	17.505		x			
SE0035R	Vindeln	64.25	19.77					x
SE0053R	Rickleå	64.167	20.933		x			
SE0093R	Abisko	68.350	18.817		x			
SE0094R	Ammarnäs	65.967	16.200		x			
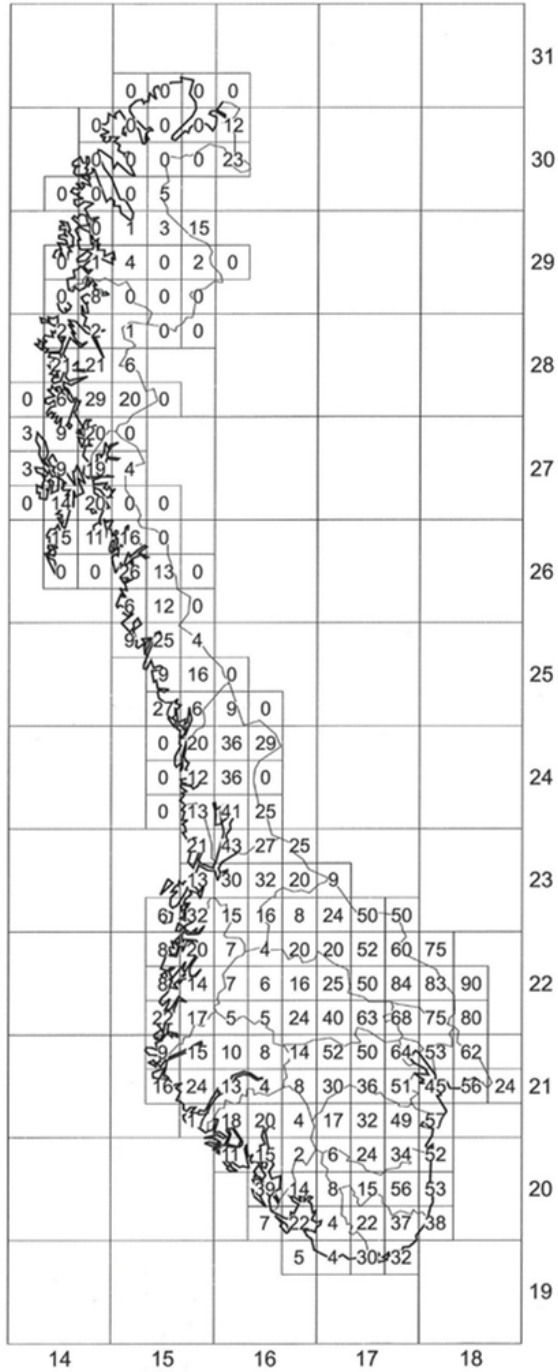
Figure S1: Percent productive forest used in estimating dry deposition to the 50×50 km^2 EMEP grid cells.

Norway - 2021
monthly data

		2Dprecip	3Dprecip-20L	3Dprecip-20L-cloudj	3Dprecip-21L	2Dprecip-NordicAnalysis
NO2	EEA-rural	77.5	80.5	80.2	89.8	38.7
	EBAS	73.7	77.4	74.1	84.7	74.5
O3Max	EEA-rural	10.8	9.8	12	8.5	11.1
	EBAS	9.1	8.1	10.1	6.7	9.3
OX	EBAS	19.9	18.9	20.3	18.1	20
SO2	EEA-rural					
	EBAS	-23.9	-21.4	-1.4	-0.2	-13.1
CO	EBAS	-11.7	-11.5	-11.7	-11.3	-11.8
PM2.5	EEA-rural	-39.8	-37.4	-39.6	-36.6	-40.9
	EBAS					
PM10	EEA-rural	-20	-16.7	-19.9	-16.7	-19.3
	EBAS	3.7	7.7	4.1	3.3	11.6
SO4	EBAS-m	-7.6	-5.5	-15.8	-17.1	9
	EBAS-d	-7.6	-5.5	-15.8	-17.1	9
NH3	EBAS-m	-74.1	-73.3	-73.1	-72	-74.8
	EBAS-d	-74.1	-73.3	-73.1	-72	-74.8
NH4	EBAS-m	32.2	39.8	31.1	33.6	52.7
	EBAS-d	32.2	39.8	31.1	33.6	52.7
HNO3	EBAS-m	110.3	124.3	128.3	113.2	113.6
	EBAS-d	110.3	124.3	128.3	113.2	113.6
NO3 PM10	EBAS-m	40.5	44.6	43	46	62.2
	EBAS-d	40.5	44.6	43	46	62.2
SS PM10	EBAS-m	3.7	11	5.4	4.5	16
	EBAS-d	3.7	11	5.4	4.5	16
EC PM2.5	EBAS-m	-38.7	-36.8	-38.1	-36.6	-43.5
OC PM2.5	EBAS-m	-14.4	-12.8	-11.7	-13.6	-11.8
WetOXS	EBAS-m	-50.8	-46.8	-49.9	-49.8	-56.3
	EBAS-d	-54.6	-50.8	-54.2	-54.2	-57.5
WetRDN	EBAS-m	-50.5	-49.1	-50.3	-50.4	-57.1
	EBAS-d	-60	-58.7	-60.2	-60.2	-66.6
WetOXN	EBAS-m	-9.9	-6.7	-6.4	-6.3	-23
	EBAS-d	-27	-24.3	-24.8	-24.8	-38.4
AOD	AERONET	57.2	55.5	53.5	50.8	67.4
Precipitation	EBAS-m	18.8	18.7	18.7	18.7	-3.6
	EBAS-d	-3.2	-3.2	-3.2	-3.2	-21.8

NMB (%)
100
50
0
-50
-100

Figure S2: Overall model evaluation for Norway in 2019. Each column is one test of the precipitation data set. The values shown are normalized mean bias.

Figure S3: Overall model evaluation of correlations with observations for Norway in 2019. Each column is one test of the precipitation data set. The values show are correlations over space.

Norway - 2021

monthly data

		2Dprecip	3Dprecip-20L	3Dprecip-20L-cloudj	3Dprecip-21L	2Dprecip-NordicAnalysis
NO2	EEA-rural	0.77	0.8	0.8	0.87	0.91
	EBAS	0.46	0.47	0.48	0.49	0.49
O3Max	EEA-rural	0.81	0.81	0.78	0.81	0.82
	EBAS	0.79	0.79	0.76	0.78	0.79
OX	EBAS	0.67	0.68	0.64	0.68	0.68
SO2	EEA-rural					
	EBAS	0.19	0.21	0.16	0.19	0.2
CO	EBAS	0.83	0.83	0.84	0.84	0.83
PM2.5	EEA-rural	0.85	0.89	0.88	0.96	0.92
	EBAS					
PM10	EEA-rural	0.65	0.65	0.69	0.75	0.6
	EBAS	0.63	0.63	0.62	0.59	0.62
SO4	EBAS-m	0.88	0.9	0.89	0.89	0.88
	EBAS-d	0.88	0.9	0.89	0.89	0.88
NH3	EBAS-m	0.4	0.38	0.31	0.3	0.39
	EBAS-d	0.4	0.38	0.31	0.3	0.39
NH4	EBAS-m	0.65	0.65	0.65	0.66	0.57
	EBAS-d	0.65	0.65	0.65	0.66	0.57
HNO3	EBAS-m	0.65	0.66	0.65	0.65	0.66
	EBAS-d	0.65	0.66	0.65	0.65	0.66
NO3 PM10	EBAS-m	0.76	0.7	0.69	0.69	0.76
	EBAS-d	0.76	0.7	0.69	0.69	0.76
SS PM10	EBAS-m	0.58	0.58	0.57	0.56	0.62
	EBAS-d	0.58	0.58	0.57	0.56	0.62
EC PM2.5	EBAS-m	0.79	0.79	0.79	0.79	0.8
OC PM2.5	EBAS-m	0.89	0.89	0.9	0.9	0.9
WetOXS	EBAS-m	0.65	0.73	0.71	0.7	0.75
	EBAS-d	0.9	0.89	0.91	0.91	0.9
WetRDN	EBAS-m	0.59	0.55	0.56	0.55	0.56
	EBAS-d	0.7	0.7	0.62	0.62	0.72
WetOXN	EBAS-m	0.8	0.79	0.79	0.8	0.76
	EBAS-d	0.81	0.81	0.79	0.79	0.75
AOD	AERONET	0.27	0.3	0.34	0.31	0.27
Precipitation	EBAS-m	0.81	0.81	0.81	0.81	0.86
	EBAS-d	0.86	0.86	0.86	0.86	0.93

R-Temporal
1
0.75
0.5
0.25
0

Figure S4: Overall model evaluation for Norway in 2019. Each column is one test of the precipitation data set. The values shown are correlations over time.
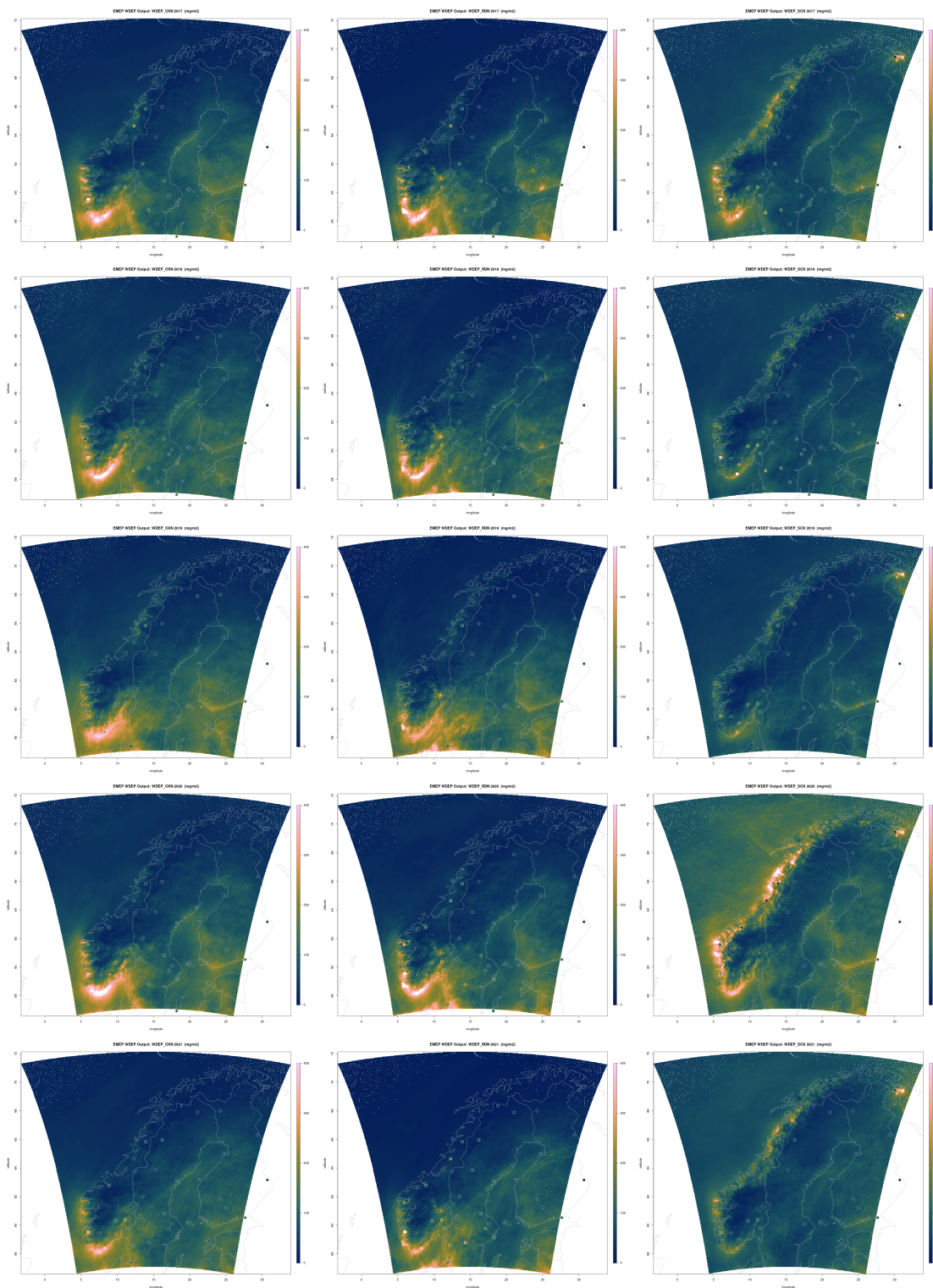
Figure S5: EMEP model output for wet deposition of NOx, NHx, and SOx over 2017 - 2021 with observations at stations superimposed. Chemical species are given in columns (From left: OXN, RDN, SOX), and each row corresponds to a year. All scales range from 0 to 400 mg/m².
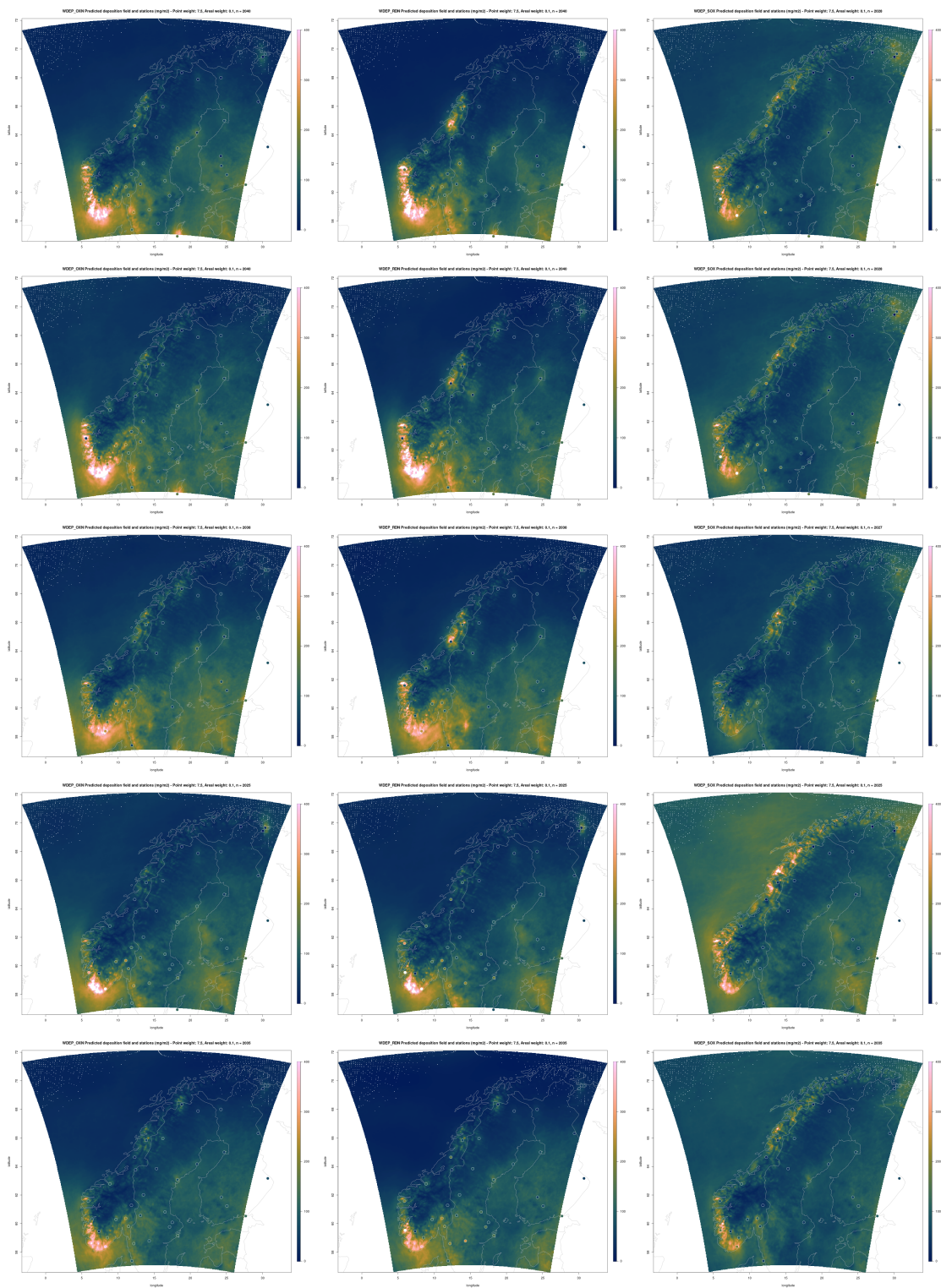
Figure S6: Fused wet deposition fields for NOx, NHx, and SOx over 2017 - 2021 with observations at stations superimposed.
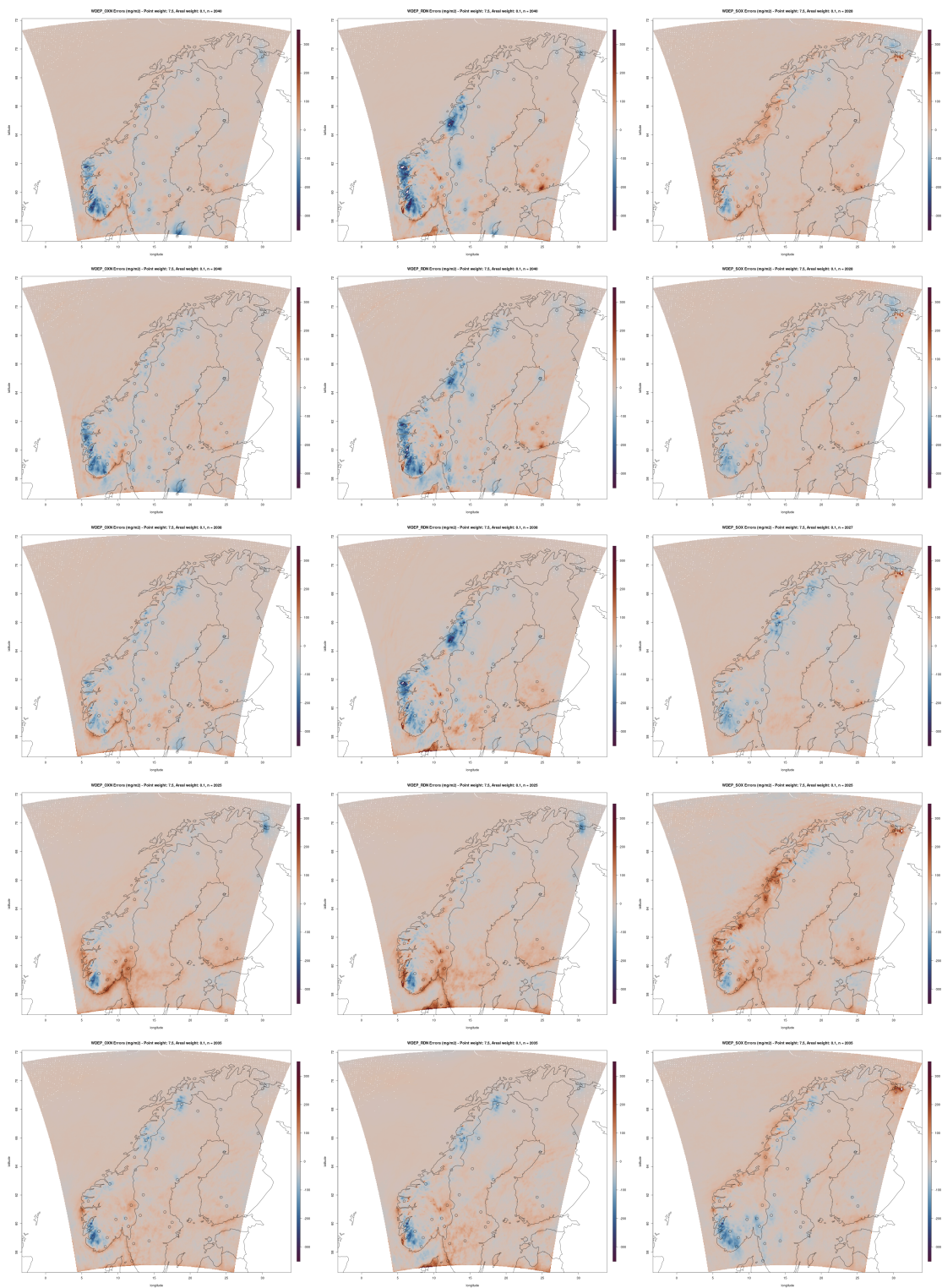
Figure S7: Differences between the fused wet deposition and EMEP model output over 2017 - 2021. Chemical species are given in columns (From left: NOx, NHx, SOx), and each row corresponds to a year. All scales range from 0 to 400 mg/m².
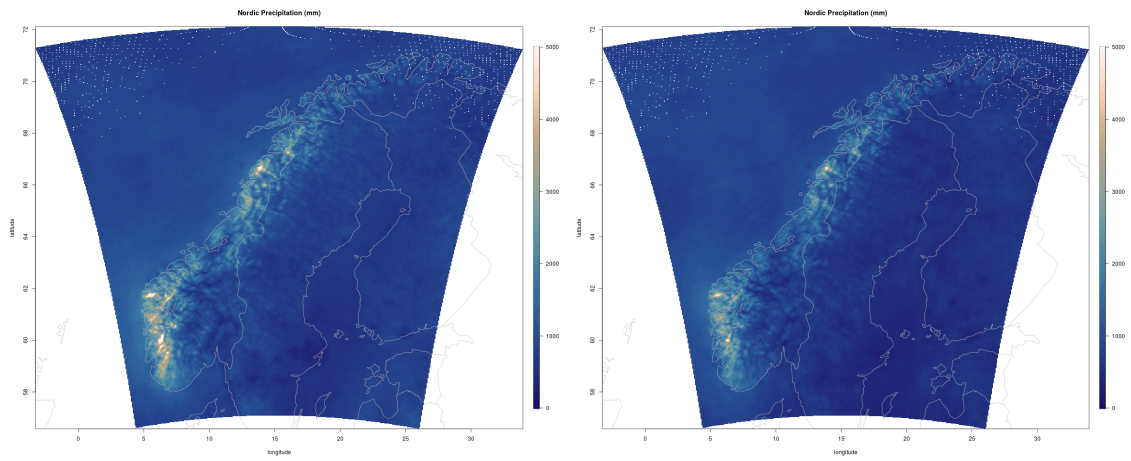
(a) 2017

(b) 2018
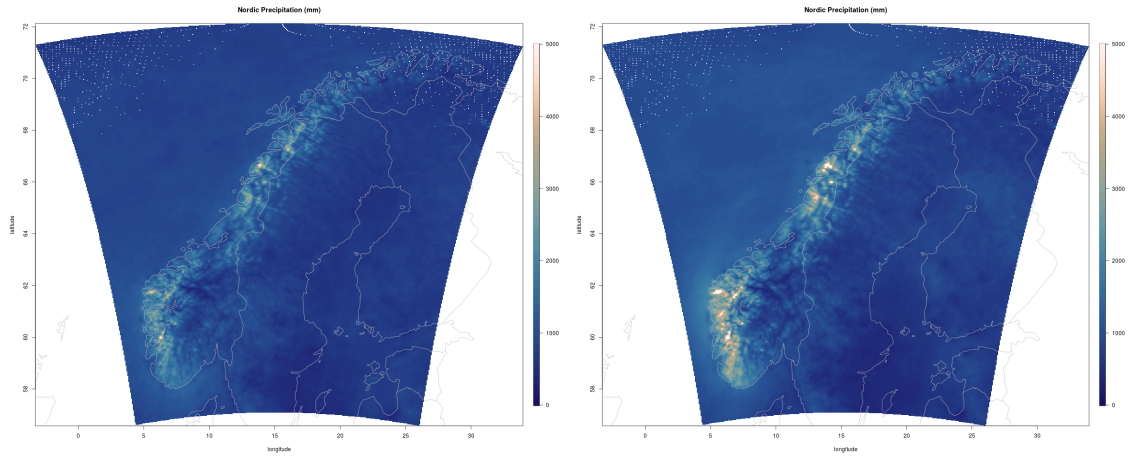
(c) 2019

(d) 2020
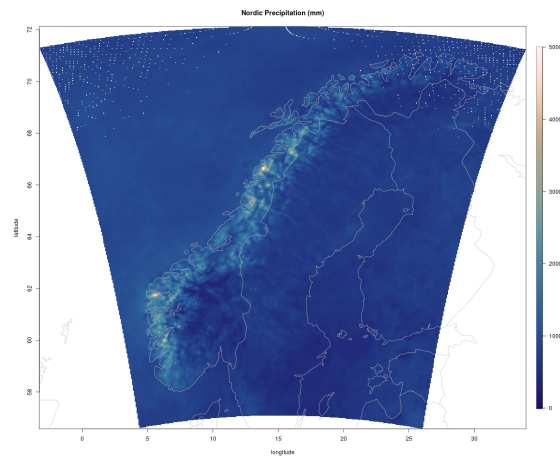
(e) 2021

Figure S8: Nordic analysis precipitation (mm) data over 2017 - 2021